Sensing and Bio-Sensing Research 29 (2020) 100373

Contents lists available at ScienceDirect

Sensing and Bio-Sensing Research

journal homepage: www.elsevier.com/locate/sbsr

Real-time optical sensing of exhaled acetone concentration utilizing non-Fickian Nafion diffusion inside a flow-through sample chamber

Ulzii-Orshikh Badmaarag[a], Data curation,Formal analysis,Investigation,Writing original draft
Jonathan A. Bernstein[b], Conceptualization,Methodology,Resources,Writing review & editing
Reza Shekarriz[c], Conceptualization,Writing review & editingAnastasios P. Angelopoulos[a,*] Conceptualization,Data curation,Formal analysis,Funding acquisition,Methodology,Project administration,Resources,Supervision,Validation,Writing review & editing

[a] Department of Chemical and Environmental Engineering, University of Cincinnati, Cincinnati, OH 45221, USA.
[b] Department of Internal Medicine, Division of Immunology, College of Medicine, University of Cincinnati, Cincinnati, OH 45221, USA.
[c] Exhalix, LLC, Albuquerque, NM 87110, USA.

ARTICLE INFO

Keywords:
Breath analysis
Optical sensor
Real-time
Nafion
Acetone

ABSTRACT

Rapid in-situ chemical analysis of flowing gas streams is of interest in a wide range of applications but requires deconvolution of the time-scales associated with the analyte source concentration, its accumulation within a sampling chamber, and its detection by a sensor. A mathematical analysis is presented on the use of a flow-through sample chamber for rapid, in-situ breath analysis utilizing analyte diffusion through a Nafion membrane optode. We show that this approach yields *apparently* non-Fickian (anomalous or Case II) transport that varies from $t^{1/2}$ to t as $t \rightarrow 0$ with constant inlet concentration. Such behavior arises due to the transition from membrane-limited to sample chamber-limited transport dynamics depending on test conditions. The model is validated utilizing experimental data obtained from the color response associated with the Friedel-Craft acylation of acetone vapor with resorcinol reagent immobilized in Nafion membrane solid-state catalyst. Reduction of optode membrane thickness and increase in membrane humidification yield an optical response limited only by sample chamber material accumulation. At this limit, the exhaled breath signal for acetone obtained from a healthy individual is found to vary as t^2 (apparently Super Case II transport). Utilizing a simplified material balance on the human lung, this observation is ascribed to a constant acetone exhalation rate as opposed to a constant exhaled acetone concentration. This conclusion is shown to have broad implications on the use of exhaled breath biomarkers for medical diagnosis, in particular, lung physiology and permeability.

1. Introduction

There is a growing need for rapid, real time (in-situ) chemical analysis of flowing gas streams in a broad range of applications including process control, material characterization, environmental hazard detection, and biomarker monitoring in exhaled breath. Practical measurements must take into account three dynamic processes that are associated with the overall signal that is observed: 1) the time-dependence of the analyte source stream, 2) the accumulation rate in the sampling chamber, and 3) the sensor response time.

Many innovative approaches for portable detection and rapid sensor response have been developed [1–4]. These typically rely on the analysis of a collected sample (i.e., an accumulated concentration) or have yet to be integrated into a practical sampling device. Without a-priori knowledge of the time-scales of these three dynamic processes, interpretation of the implications of the signal obtained can be deceptive. For example, the equilibrated sensor signal obtained ex-situ from a total amount of material collected in a bag at a given flow rate can be used to obtain the concentration of the source stream sans other information only if this concentration is constant (time-independent). By contrast, in-situ determination of the inlet concentration in real time, even if constant, will require evaluation of the dynamics of the individual processes involved. Until steady state is reached, the rate of material accumulation in the analysis chamber will convolute with the dynamics of the detection method being used (e.g., membrane diffusion) and the time dependence of the inlet concentration. Depending on the

* Corresponding author.
E-mail address: angeloas@ucmail.uc.edu (A.P. Angelopoulos).

https://doi.org/10.1016/j.sbsr.2020.100373
Received 24 April 2020; Received in revised form 26 July 2020; Accepted 29 July 2020

application, steady-state may never be reached on the required time-scale of the measurement. This is particularly the case when the flow source is limited, as during human breath exhalation, or when rapid detection is desired due to the toxicity of the analyte in the ambient.

In this paper, we demonstrate how the time scale of an chemical sensor response based on analyte diffusion into a membrane can be sufficiently reduced so as to probe sample chamber accumulation dynamics for an inlet concentration that is either constant or has a linear time dependence. These cases are shown to be particularly relevant to analysis of exhaled breath acetone concentration. Exhaled acetone has been repeatedly correlated to blood biomarkers such acetoacetate and β-hydroxybutyrate that are associated with diabetes mellitus (DM) [5]. However, exhaled breath acetone correlation to blood glucose is often not as highly resolved [5–7]. We discuss how correlation of breath acetone measurements to blood glucose can potentially be improved through more careful consideration of the impact that mass transport parameters, such as lung physiology, have on the dynamic evolution of the sensor response. Given that a typical breath exhalation can be sustained no longer than ~40 s, acetone sensing methods require time resolution on the order of 1 s to be able to deconvolute the time-scales of the mass transport processes involved. Existing portable detection methods have yet to achieve such time resolution and rely on ex-situ analysis of a collected breath sample. Examples of such an approach include the pre-concentration of breath sample into an absorbate for subsequent elution to a sensor [8], trapping exhaled breath in gas analysis chamber to accommodate a delayed sensor response [9], as well as collection in a bag for subsequent analysis [5]. These methods cannot capture the dynamics of the source material.

We have previously shown how the optical response arising from chemical reaction between reagent molecules immobilized within Nafion® membrane and volatile gases can be used for highly selective, sensitive (sub-ppb), and rapid detection suitable for in-situ measurement [10,11]. In the case of acetone, the specific sensing mechanism involves the condensation reaction of ambient acetone with membrane-immobilized resorcinol to produce a flavan with highly selective optical characteristics in the visible range of the electromagnetic waves. The product has a characteristic absorbance peak at 400.7 nm. The reaction is depicted in Scheme 1. A diffusion-limited time resolution within 1 s has been observed utilizing our membrane catalyst approach, opening the possibility of in-situ, real time chemical analysis of human breath. Acetone membrane diffusion in our previous investigations was found to be Fickian at ppm concentrations relevant to breath analysis [10,12].

Interferences from molecules such as ethanol and carbon monoxide have previously shown to be non-existent as they are incapable of undergoing an acid-catalyzed reaction with resorcinol. In addition, water interference due to de-protonation of the perflurosulfonic acid group has been eliminated through the immobilization of weak organic acids which create a mixed-solvent system when water is present. Other volatile organic breath components are found to be present at far lower concentrations and do not convolute the spectral response to acetone.

Despite these scientific advances, practical application of the membrane catalyst approach to real-time, in-situ breath analysis requires that the membrane be incorporated into a macroscopic interface such as a flow-through sample chamber for patient use. The impact of chemical composition in a flow-through sample chamber on membrane diffusion has never been previously investigated. Such in-situ analysis is important not only to reduce the lag time associated with patient feedback but, on a more fundamental level, to determine the dynamics of acetone evolution in the lungs. Solution to this problem will find additional application in scenarios where an acute environmental exposure must be rapidly assessed as in the case of occupational hazards, process control scenarios, or chemical warfare agents.

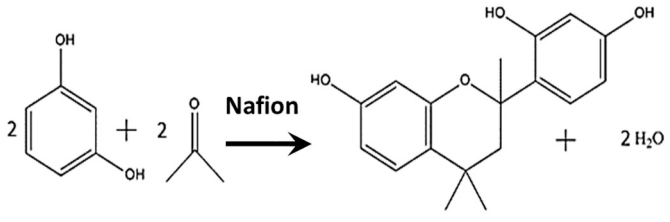

Scheme 1. Nafion®-catalyzed condensation reaction with resorcinol used for optical detection of acetone.

The objective of this investigation is to model the kinetics of species transport through a membrane confined inside a flow through sample cell typical of the system used in our studies. We will show that the observed optical response can, under appropriate system conditions, exhibit *apparently* non-Fickian transport behaviors [13,14]. The model will be confirmed through calibration experiments and key membrane parameters extracted in order to help with detection optimization and data interpretation.

2. Experimental

Nafion® membrane (The Fuel Cell Store, Nafion® 117, protonated, 0.007 in. thickness, 1100 EW) was used as received and immersed in a 12 g L^{-1} solution of resorcinol (Acros Organics, 98%) in ethanol (Acros Organics, ACS spectroscopic grade, > 95% purity) for 31 min as described in further detail in our previous work. The membranes were rinsed with deionized water and allowed to air dry. The membranes were then placed into a flask containing 50 g L^{-1} of tiglic acid (TA, Sigma-Aldrich, > 98%) in heated food grade mineral oil (Bayes, 100%).

Mineral oil was utilized to avoid loss of the resorcinol in the membrane during the organic acid uptake. The membranes were soaked in the solution for 1 to 24 h depending on the rate of uptake observed and then the excess oil solution was rinsed off and the membrane allowed to air dry. Extraction of the organic acids in ethanol and Beer-Lambert's Law were used to quantify the amounts of the acids that had been imbibed into the membrane.

To investigate the evolution of the optical signal in a flow-through sample chamber in real time, a custom-built system was developed as shown in Figs. 1 and 2. This system allowed us to control the volume of flow-through analysis chamber (13.5 mL) in place of the quartz cuvette utilized in our previous work (2.5 mL) [10]. As will be demonstrated in this study, reduction of analyte diffusion resistance in the membrane optode in favor of its accumulation in the sample chamber is essential to accurately model inlet stream dynamics. This system also employs a less expensive, more compact, and more durable color sensing technology to assess optode response instead of a UV/Vis Spectrophotometer.

The membrane optode is placed onto a clamshell fixture which is then inserted into the sample chamber at the system casing opening shown in Fig. 1(a). The inlet flow tube is inserted into the position indicated in Fig. 1(a). The compact and durable system casing is convenient for travel to and from clinical trials, as shown in Fig. 1(b). Custom software was prepared to monitor and save the optical response as well as provide a color eye-guide on a computer screen for patients to achieve control over their exhalation rate. The computer screen as viewed by patients is shown in Fig. 1(c). The exhalation rate which proved most comfortable with patients was between 1.5 and 2.0 L min^{-1}. This was monitored continuously during the experiment utilizing the flow meter which forms part of the internal system components as shown in Fig. 2.

The color sensing approach is described schematic in Fig. 1(d) and achieved utilizing the commercial color reader shown in Fig. 2. A white-light LED provides the light source. An array of > 300,000 pixels records an image by collecting the reflected light in RGB. Each pixel on the sensor has a color filter that only lets in one color. The captured image records the brightness of each color separately. Only the blue absorbance is used for measurement of flavan product formation.

Resistance heating and microprocessor control as shown in Fig. 2 are used to bring the temperature of the sample cell to the 60 °C

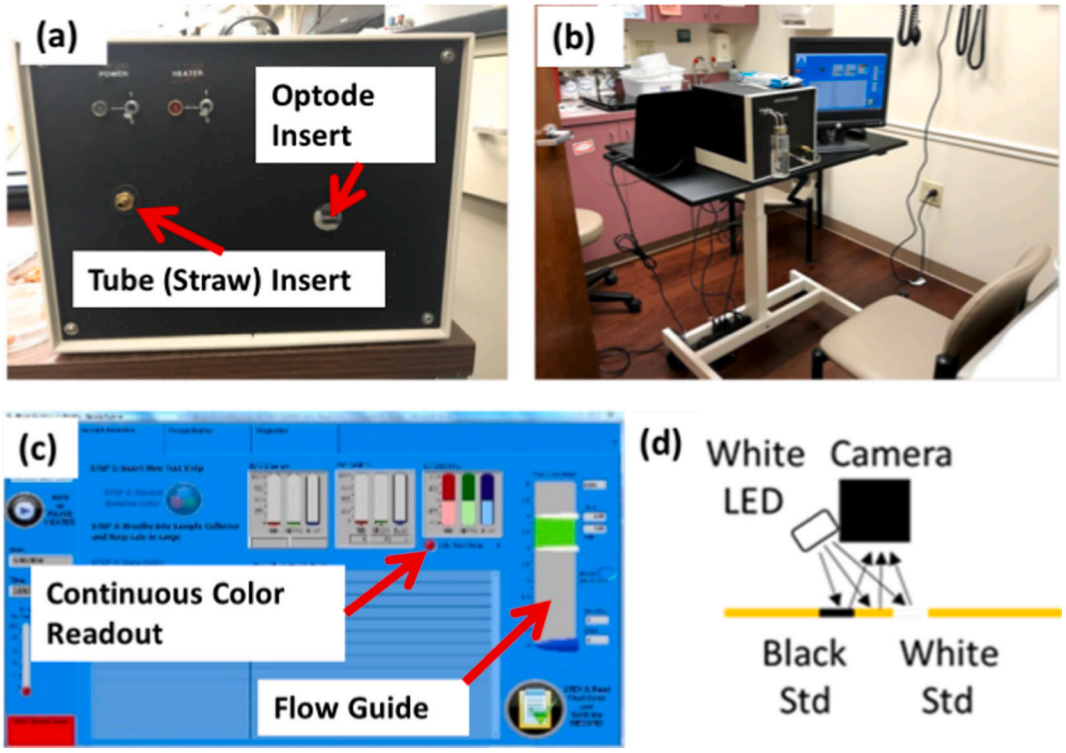

Fig. 1. Flow-through sampling system. (a) Durable casing used to transport system to and from clinical trials. (b) System set-up at clinician's office. (c) Software interface for patients and operator. (d) Color measurement scheme.

reaction temperature. A small pump provides a dry air purge which could be manually switched to go through a water bottle for humidification as desired.

Gas standards for device calibration were prepared by bubbling dry air over acetone and then diluting with another dry air stream to desired concentration prior to humidification (as desired).

For the exhaled breath clinical trials performed for this work, the inlet flow tube was replaced by a straw at the position shown in Fig. 1(a). Subjects without a history of physician diagnosed DM or chronic respiratory disease (i.e., asthma) were randomly recruited from a large community medical practice, as shown in Fig. 1(b). Subjects were tested as they became available throughout the day. After signing an informed consent approved by the University of Cincinnati Institutional Review Board, each subject was asked to clear their lungs with a deep inhale and exhale and then, after taking a deep breath, exhale into the straw for as long as possible. The subjects were asked to maintain an exhalation rate of 2 L min^{-1} utilizing the eye-guide on the computer screen shown in Fig. 1(c). Flow rate was monitored and recorded by the meter indicated in Fig. 2. Subjects were allowed one or two practice trials to control their exhalation rate before the optode was inserted. Blood glucose measurements were obtained by the nursing staff both before and after at least two trials conducted in this manner. All patients who participated were in a nonfasting state but had not eaten within an hour prior to testing.

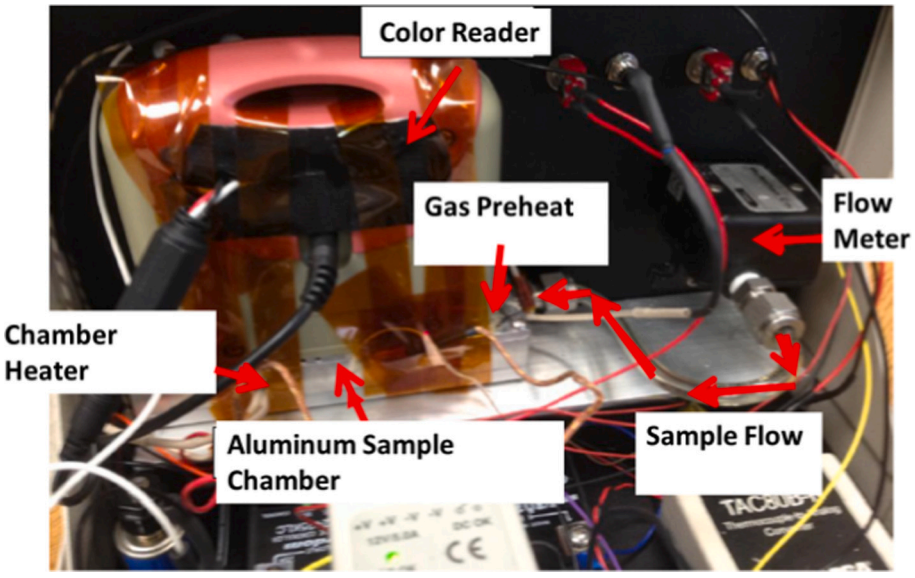

Fig. 2. Internal view of flow sampling system.

3. Results and discussion

3.1. Theory with constant inlet concentration

3.1.1. Sample chamber accumulation

Fig. 3 depicts the basic flow through sample-cell arrangement and associated parameters of interest.

In Fig. 3, C_{in} is the initial inlet concentration, C_{out} is outlet concentration, ν_{in} and ν_{out} are the corresponding inlet and outlet volumetric flow rates, and V_s is the sample chamber volume.

Assuming that there is no leak in the sample chamber, the corresponding sample chamber volume V_s remains constant for the entire path, and that the chamber is well-mixed at a uniform species concentration $C = C_{out}$, a mass balance of the system yields:

$$V_s \frac{dC}{dt} = \nu_{in} C_{in} - \nu_{out} C \tag{1}$$

Accumulation of material in the sample chamber will provide the membrane boundary conditions required for mathematical determination of species uptake in the membrane located inside the chamber. We note that ν_{out} in Eq. (1) will be time-dependent due to the development of a pressure drop to drive flow. The precise functional form of ν_{out} will depend on the details of the sample chamber design, including materials of construction. To generalize our approach, we recognize that during the taking of initial measurements, the last term on the right in the material balance will be negligible. In other words, to $O(C\nu_{out}/C_0\nu_{in}) \rightarrow 0$, the solution of Eq. (1) becomes, where we set $\nu = \nu_{in}$:

$$C = \frac{\nu\, C_0}{V_s}\, t \tag{2}$$

For the sampling system employed in this work, parameter ν/V_s has a value of 2.46 s^{-1} at a flow of 2 L min^{-1} versus a value of 13.1 s^{-1} for the quartz cuvette flow through system previously found to exhibit an optical response limited by Fickian transport through the optode [10].

For the given concentration accumulation in the sample chamber given by Eq. (2), the time dependence of the optical signal will be convoluted by partitioning of acetone into the membrane optode. The two limiting cases where optical detection is limited by sample chamber dynamics or membrane resistance are discussed.

3.1.2. Membrane transport as rate-limiting step

If transport through the membrane at early times limits transport, then the sample chamber will reach a uniform concentration of C_0 prior to optical signal detection. In this case, then the solution for the weight uptake per unit area, M_t, at early times is given by [15]:

$$M_t = 4\, H\, C_0 \left(\frac{Dt}{\pi}\right)^{1/2} \tag{3}$$

where D is the (constant) acetone diffusion in the membrane and H is the membrane partition coefficient. The concentration, C_m, in the membrane at any time may be expressed according to: $C_{m,t} = M_t/L$, where L is the membrane thickness.

We next apply the Beer-Lambert Law to relate the membrane concentration to the absorbance signal, A_t, according to:

$$A_t = \varepsilon\, L\, C_{m,t} \tag{4}$$

where ε is the extinction coefficient.

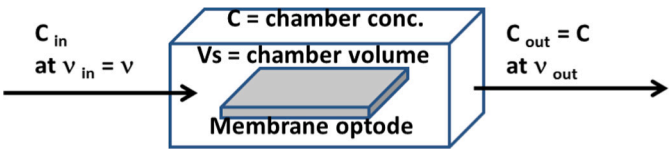

Fig. 3. Sample chamber model illustrating material balance terms.

Eq. (3) may therefore be re-written as:

$$A_t = 4\, \varepsilon\, H\, C_0 \left(\frac{Dt}{\pi}\right)^{1/2} \tag{5}$$

Such behavior is categorized as Fickian diffusion [13].

3.1.3. Sample chamber accumulation as rate limiting step

In the case where membrane transport is much more rapid than sample chamber dynamics, then we can write directly from Eqs. (2) and (4) that:

$$A_t = \left(\frac{\varepsilon\, L\, H\, C_0\, \nu}{V_s}\right) t \tag{6}$$

Such behavior is categorized as Case II sorption [13,14] but is here only apparently so because it arises due to sample chamber-limited accumulation.

3.1.4. Analysis of experimental data

If independently-determined solubility, H, and diffusivity, D, data is not available, then the product of membrane parameters observed in Eqs. (5) and (6) cannot be de-convoluted and quantitative chemical sensing must be achieved through calibration measurements. In this case, we re-write Eqs. (5) and (6) according to:

$$A_t = B_n\, C_0\, t^n \tag{7}$$

where n takes on the value of ½ (Fickian diffusion) or 1 (apparently Case II sorption), respectively, and B_n has the corresponding convoluted product of membrane and system parameters.

To evaluate experimental data, Eq. (7) may be recast in the form:

$$\ln(A_t) = \ln(B_n\, C_0) + n \ln t \tag{8}$$

Which limiting case is operative for a given set of operating conditions can therefore be inferred from the value of n obtained by plotting ln (A_t) versus ln t. The value of B_nC_0 for a given inlet chamber concentration C_0 is obtained from the intercept of such a plot. Therefore, calibration consists of plotting this value for various known concentrations, C_0 (including $A_t = 0$ at $C_0 = 0$) to extract the convoluted parameter product, B_n. Measured absorbance dynamics may then be used to extract an unknown concentration C_0.

In addition to being essential for point-of-care applications, such an early time approach avoids the need for separate ex-situ (off-site) experiments to obtain extinction coefficient, membrane optode, or system configuration parameter data.

Intermediate values of n between ½ and 1 are anticipated from Eq. (8) when the limiting cases are not fully satisfied in the experimental data collected. Such behavior is typically categorized as anomalous diffusion but here arises due to the convolution of membrane-limited and sample-chamber limited transport [13,14]. While n may remain stable and permit system calibration under a given set of operating conditions, it is important to note that the relationship between B_n and system parameters is uncertain in those situations.

The applicability of this approach hinges on both the Fickian nature of transport through the membrane at early times as well as whether parameter $C\nu_{out}/C_0\nu_{in}$ is sufficiently small so that Eq. (2) applies.

We will illustrate application of these concepts to experimental data in the following section.

3.2. Experimental UV–vis measurements

3.2.1. Calibration data

We have previously noted that the condensation reaction shown in Scheme 1 readily equilibrates in homogeneous aqueous solution in a matter of seconds. Consequently, the optical response in Nafion® membrane is limited by diffusion of acetone to the immobilized reagent/catalytic sites.

In Fig. 4, we show dynamic response data obtained with a 7 mil

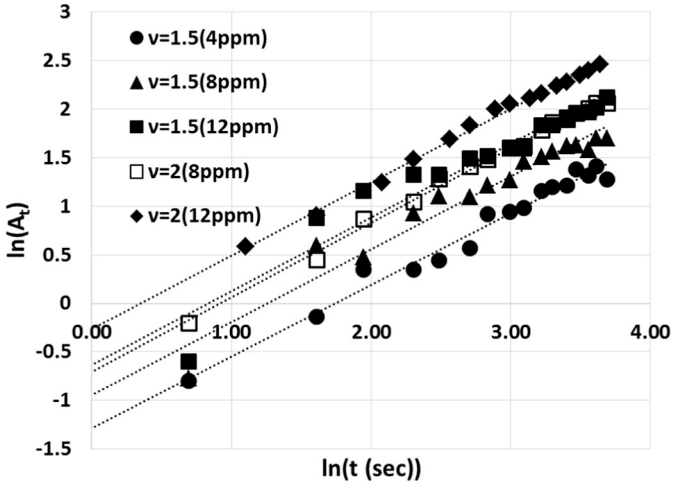

Fig. 4. Natural logarithm plot of the absorbance versus time in seconds obtained at the indicated inlet concentration in ppm and the indicated flow rate in L min^{-1}, either 1.5 or 2.0. Dry purge and 7 mil optode test conditions. A slope of 0.75 +/− 0.011 is obtained from all lines, indicating an intermediate case of mass transport where neither membrane diffusion nor sample chamber accumulation is rate limiting.

Nafion membrane purged with dry air both before and after exposure to fully humidified acetone at the indicated constant exposure levels at the indicated volumetric flow rates at the inlet of the sample chamber. These are plotted according to Eq. (8).

From Fig. 4, we obtained a value of 0.75 for n with a standard deviation of +/− 0.011 for every exposure and flow rate, indicating an intermediate case between membrane control and sample chamber control for this system. This suggests that neither membrane transport nor sample chamber accumulation is rate limiting.

A plot of BC_0 versus C_0 from this data is shown in Fig. 5 and yields $B_{0.75}$ values of 0.0633 +/− 0.0010 ppm^{-1} $s^{-0.75}$ at 2 L min^{-1} and 0.0473 +/− 0.0045 ppm^{-1} $s^{-0.75}$ at 1.5 L min^{-1}. Although the ratio of these two values is consistent with that expected from the flow rates, the linear fit to the 1.5 L min^{-1} data is very poor, with a correlation coefficient of $r^2 = 0.73$. This is shown in Fig. 5(a).

We next investigated the impact of humidifying the membrane prior to exposure by first injecting a fully humidified purge stream for 5 min. Note that while both the purge and exposure streams are fully humidified at ambient laboratory temperature, the humidification is reduced to about 16% at the 60 °C reacting temperature of the sample chamber. Furthermore, the high solubility of acetone in water would mitigate transport resistance due to the presence of a condensed layer. The impact of this change is shown in Fig. 6.

Fig. 6 indicates that pre-humidifying the sample chamber has the effect of reducing membrane resistance. This is noted from the reduced slope on the data relative to the dry purge employed in Fig. 4. The value of n for all lines in Fig. 6 is 0.89 +/− 0.027. The slope $B_{0.89}$ has a value of 0.0428 +/− 0.0026 ppm^{-1} $s^{-0.89}$ at a flow of 2 L min^{-1} and 0.0282 +/− 0.0012 ppm^{-1} $s^{-0.89}$ at a flow of 1.5 L min^{-1}, as shown in Fig. 5. While the correlation coefficients for this calibration are improved, the ratios at the two flow rates are not consistent with sample chamber-limited transport.

To further reduce membrane resistance, we prepared optodes utilizing a 1 mil membrane. We maintained a fully humidified purge stream at ambient prior to exposure and obtained the data shown in Fig. 7.

The value of n obtained from each linear fit in Fig. 7 is 1.0 +/− 0.017. This value suggests that the optical response is being driven by the dynamics of sample chamber accumulation. The slope $B_{1.0}$ has a value of 0.0442 +/− 0.0015 ppm^{-1} s^{-1} at a flow of 2 L min^{-1} and

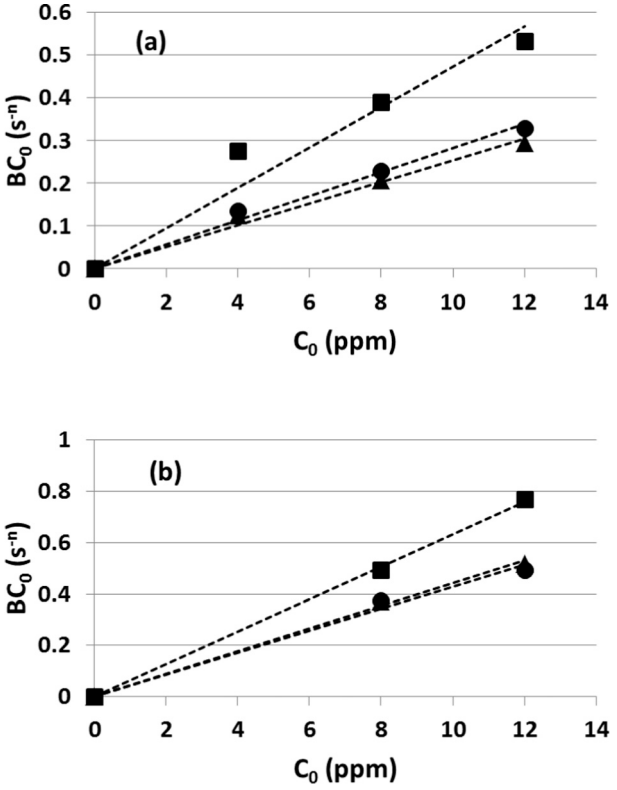

Fig. 5. BC_0 versus C_0 for dry purge condition and 7 mil membrane (squares), humid purge condition and 7 mil membrane (circles), and humid purge condition and 1 mil membrane (triangles). Force-fit through origin. (a) 1.5 L min^{-1}. (b) 2.0 L min^{-1}.

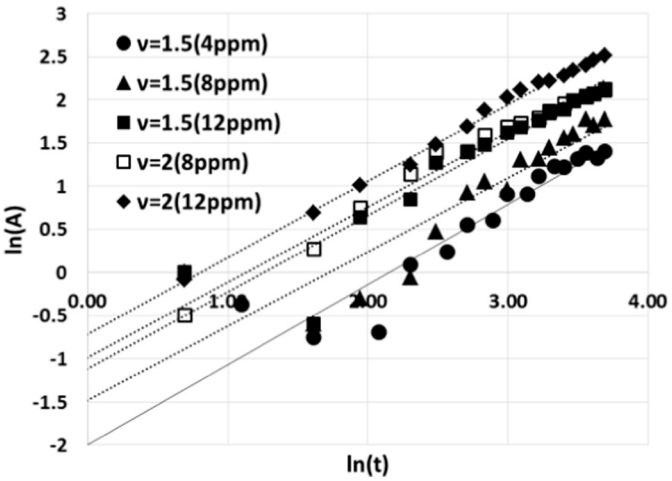

Fig. 6. Natural logarithm plot of the absorbance versus time in seconds obtained at the indicated inlet concentration in ppm and the indicated flow rate in L min^{-1}, either 1.5 or 2.0. Humidified purge and 7 mil optode test conditions. A slope of 0.89 +/− 0.027 is obtained from all lines, indicating a reduction in membrane mass transport resistance due to increased humidification.

0.0254 +/− 0.0012 ppm^{-1} s^{-1} at a flow of 1.5 L min^{-1}, as shown in Fig. 5. The ratio of these values is even less consistent with the flow rates than those obtained with the thicker membrane, despite being obtained from excellent fitting (see Fig. 5). This observation suggests that the level of membrane humidification in the 60 °C flow chamber is flow-rate dependent, particularly with the thinner membranes, and will therefore impact the extent of acetone partitioning into the membrane

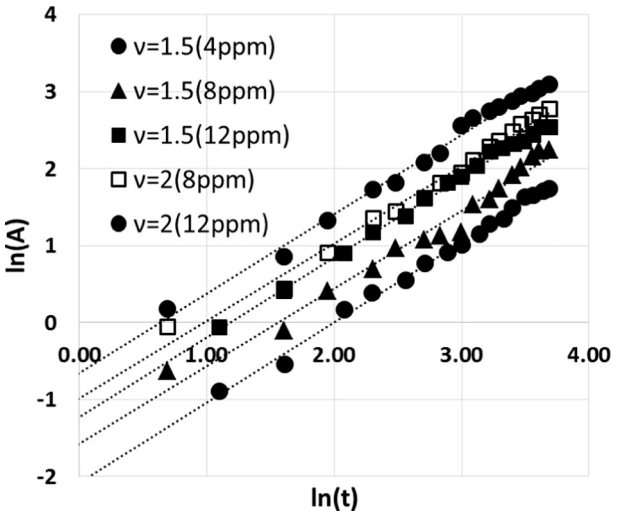

Fig. 7. Natural logarithm plot of the absorbance versus time in seconds obtained at the indicated inlet concentration in ppm and the indicated flow rate in L min^{-1}, either 1.5 or 2.0. Humidified purge and 1 mil optode test conditions. A slope of 1.0 +/− 0.017 is obtained from all lines, indicating the mass transfer is controlled by sample chamber accumulation.

(parameter H in Eq. (6)). This result emphasizes the importance of maintaining constant test conditions for appropriate calibration utilizing this optode approach. Nevertheless, humidification is sufficient to ensure that sample chamber rather than membrane dynamics are being sampled. The statistics indicate good reproducibility as long as consistent humidification conditions are maintained. Ideally, the effect of flow should be eliminated and we are investigating the use of a heated inlet purge to achieve this by increasing the humidification level in the sample chamber.

Our theoretical model for early time behavior predicts that the calculated calibration parameter B_n should be proportional to the flow rate (see Eq. (6)). However, this dependence presumes that membrane parameters remain constant as flow rate changes. The calibration plots in Fig. 5 demonstrate that, even if sample chamber accumulation were rate limiting ($n = 1$), acetone partitioning in the membrane can still exert a subtle influence on the signal that is observed. While the influence of acetone partitioning can never be eliminated, its alteration by sampling conditions can be mitigated by ensuring that the membrane is always fully humidified.

3.2.2. *In-situ measurement of exhaled acetone concentration*

The advantage of monitoring sample chamber dynamics rather than optode resistance is next illustrated during the in-situ measurement of exhaled breath concentration.

A 34 year-old female subject with an average blood glucose reading of 107 mg dL^{-1} and no health issues was instructed to blow into the sample chamber at a steady rate of 2 L min^{-1} as described in the Experimental Section. The patient achieved a minimum of 25 s of exhalation for each of the final 2 trials. The membrane optode was purged with humidified air for 5 min prior to exhalation and a 1 mil thick optode was used. Results are shown in Fig. 8, linearized according to Eq. (8).

From Fig. 8, we obtained the unexpected result that $n = 1.9 +/- 0.029$. To understand such unusual behavior, we explored the impact of acetone accumulation in the lungs on the time dependence of exhaled acetone concentration. The importance of limiting optical response to sample chamber dynamics is well-illustrated during the in-situ measurement of exhaled breath concentration. The following section provides a lung model analysis to better explain the data presented in this section.

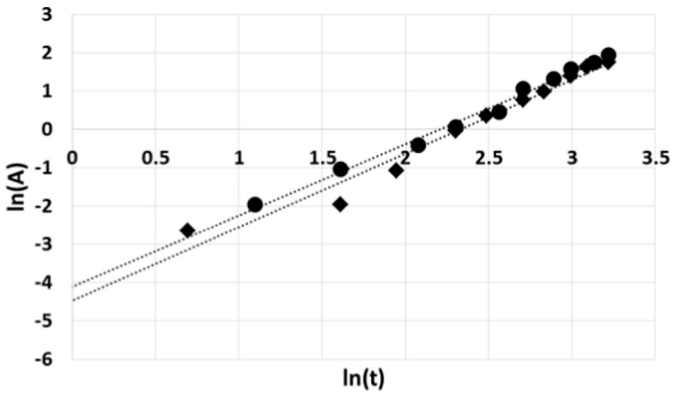

Fig. 8. Natural logarithm plot of the absorbance versus time in seconds obtained from a 34 year old female subject with 107 mg dL^{-1} average blood glucose and no health issues exhaling at 2.0 L min^{-1}. Humidified purge and 1 mil optode test conditions. A slope of 1.9 +/− 0.029, indicative of a linear time dependence in the inlet concentration to the sample chamber.

3.3. *Theoretical lung model*

A simple model of exhaled breath time dependence can be obtained by considering steady-state transport through the capillaries in the lungs as shown in Fig. 9 according to:

$$N_c = k_c (C_0 - C_{ex}) \quad (9)$$

Where N_c is the acetone mass (or molar) *flow rate* through the capillary wall into the lung volume on a gas concentration basis, considered to contain a well-mixed concentration C_{ex}, which is the concentration of acetone in exhaled breath entering the sample analysis chamber shown in Fig. 3. C_0 is the concentration of acetone in the gas phase in equilibrium with blood-acetone concentration, C_B, as expressed by a Henry's Law type of relationship shown below:

$$C_B = H_{GB} C_0 \quad (10)$$

where H_{GB} is the gas-blood acetone partition coefficient.

Parameter k_c in Eq. (9) is a generalized blood capillary wall/lung tissue mass transport coefficient expressed in its simplest form as:

$$k_c = \frac{D_c A_c H_{Bc} H_{GB}}{L_c} \quad (11)$$

where D_c is the diffusion coefficient of acetone through a tissue wall of thickness L_c and average transport area A_c. Parameter H_{Bc} is the acetone partitioning coefficient between the blood and the capillary wall/lung tissue. At equilibrium, it links the concentration of acetone in the capillary, C_c to that in the blood phase:

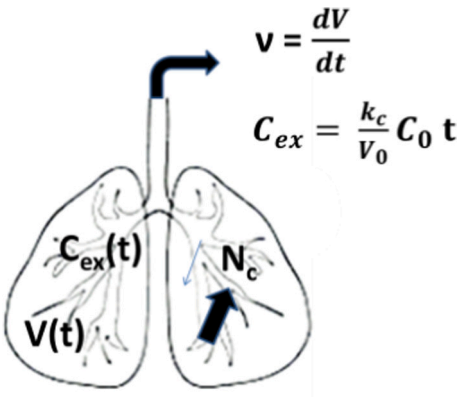

Fig. 9. Schematic of theoretical steady-state lung tissue permeation model. Parameters are defined in text.

$$C_c = H_{Bc} C_B \tag{12}$$

The material balance around the well mixed lung volume shown in Fig. 5 under forced exhalation, taking account the change in volume with exhalation rate, ν, is given by:

$$(V_0 - \nu t)\frac{dC_{ex}}{dt} = k_c(C_0 - C_{ex}) \tag{13}$$

where V_0 is the initial lung volume prior to exhalation and ν is the volumetric exhalation rate, identical to the volumetric rate input to the analysis chamber.

To both $O(\nu t/V_0 \rightarrow 0)$ and $O(k_c t/V_0 \rightarrow 0)$, Eq. (13) has the early time solution:

$$C_{ex} = \frac{k_c}{V_0} C_0 \, t \tag{14}$$

Such a linear dependence in exhaled breath concentration has not been previously reported. Employing $C_{in} = C_{ex}$ in Eq. (2) and solving at early exhalation times when:

$$\frac{\nu_{out}}{\nu}\frac{C}{C_0}\frac{V_0}{k_c} \ll t \tag{15}$$

We obtain:

$$C = \frac{1}{2}\frac{\nu}{V_s}\frac{k_c}{V_0} C_0 \, t^2 \tag{16}$$

A t^2 time dependence is therefore expected from the optical response of breath exhalation in a system which is limited by accumulation in a sample chamber. Such behavior is categorized as Super Case II Sorption [13,14] but here arises from sample chamber-limited transport and a time-dependent inlet concentration. Had the system been membrane transport limited, then the physiological lung properties responsible for the dynamic behavior could not be captured.

Applying Eq. (4) to Eq. (16) yields:

$$A_t = \frac{\varepsilon L H}{2}\frac{\nu}{V_s}\frac{k_c}{V_0} C_0 \, t^2 \tag{17}$$

Eq. (17) indicates that linearizing experimental data for exhaled breath according to the log-log plot given by Eq. (8) will yield $n = 2$ if the sample chamber dynamics are rate limiting, which corroborates the results shown in the previous section and Fig. 8 (i.e., $n \approx 1.9$).

Knowledge of the sample chamber dynamics dependence is not required to obtain the average exhaled acetone concentration over a fixed period of time. However, failure to recognize differences in lung physiology among patients can yield hopelessly convoluted results and is one likely source of discrepancies among conclusions reported in the literature. This is particularly the case with respect to correlations between exhaled breath acetone concentration and blood glucose.

3.4. Experimentally determined lung tissue permeability

From our experimental results in Fig. 8, we obtain a value of $B_{1.9}$ $C_0 = 0.0137 +/- 0.0034$ $s^{-1.9}$. We noticed during these patient trials that the theoretical value of $n = 2$ and more highly reproducible values for B_n were approached with repeated trials, suggesting improved sample chamber humidification. For a healthy patient with normal blood glucose levels, a breath acetone concentration of about 1 ppm is frequently reported [5]. Using this value for C_0, we write that $B_{1.9} = 0.0137 +/- 0.0034$ ppm^{-1} $s^{-1.9}$.

We employ the value of B_1 obtained for calibration experiments conducted under similar test conditions ($\nu = 2$ L min^{-1}, humidified purge, 1 mil membrane) and write:

$$B_2 = B_1 \frac{1}{2}\frac{k_c}{V_0} \tag{18}$$

Taking $B_{1.9} \sim B_2$ in Eq. (17) yields a value of $0.310 +/- 0.0037$ s^{-1} for k_c/V_0 with propagation of error for the patient tested.

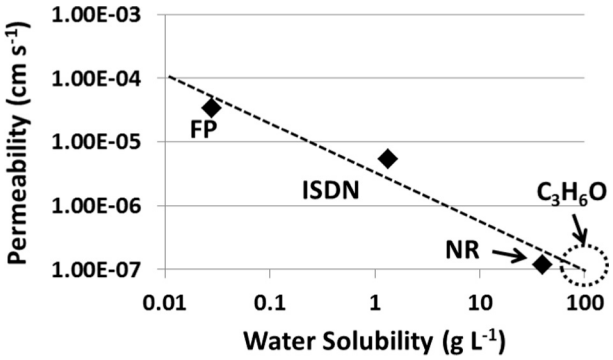

Fig. 10. Correlation of model drug permeability in Sprague Dawley rat skin and water solubility. Acetone estimate given by dotted circle.

Assessment of the validity of this number is difficult given that diffusivity and solubility data for acetone in animal tissue is not readily available. We will instead develop a correlation based on reported permeation data for various model drugs through Sprague Dawley rat skin [16]. Fig. 9 plots the permeability of Nicorandil (NR), isosorbide dinitrate (ISDN), and flurbiprofen (FP) through SD rat skin from water versus their solubility in water at RT. The dotted circle in the figure indicates our correlated acetone permeability as a basis for comparison.

We write the acetone permeability through the blood capillary wall/lung tissue resistance from water, P_{wc}, as:

$$P_{wc} = \frac{D_c H_{wc}}{L_c} \tag{19}$$

where H_{wc} is analogous to parameter H_{Bc} in Eq. (11) but accounted for acetone partitioning in water instead of blood. A comparable expression can be written for acetone permeability through the capillary wall resistance from blood, P_{Bc}, as:

$$P_{Bc} = \frac{D_c H_{Bc}}{L_c} \tag{20}$$

We use the correlation in Fig. 10 to obtain $P_{wc} \sim 10^{-7}$ cm s^{-1}. Given that the solubility of acetone in PDMS at RT is three orders of magnitude greater than that of water [17] we write: $H_{Bc} \sim 10^3 H_{wc}$ and so $P_{Bc} = \sim 10^{-4}$ cm s^{-1} at RT. We also know that acetone blood partitioning from air, H_{GB}, is ~260 at RT. Next, we use a spherical lung volume approximation and an average lung capacity of 6 L to estimate that $A_c/V_0 \sim 0.266$ cm^{-1}. Combining these approximations yields $k_c/V_0 \sim 0.01$ s^{-1} at RT or ~ 0.1 s^{-1} at the 60 °C optode temperature. That this value is about one-third that which we obtained from exhaled breath measurements is remarkable given the approximations employed. Such correspondence suggests the possibility of using this approach to discriminate both longitudinal and cross-sectional changes in lung physiology due to disease.

3.5. Preliminary data on the effect of age

A small-scale study was conducted with a random cross-section of subjects who had normal blood glucose levels (< 120 mg dL^{-1}) and no underlying conditions as described in the Experimental Section. A humidified purge was employed both before and after each trial. In addition, a 7 mil thick membrane optode was used for convenience given the comparable value of B_n that were obtained with a humidified purge and a 1 mil sample in the calibration study. Nevertheless, we found it difficult to maintain sufficient membrane humidification so as to achieve $n \sim 2$ in the plotted data with our current humidification scheme. More extensive trials with a heated humidifier are planned in the future.

To illustrate the type of real-time exhaled breath data that can be collected in a clinical setting as well as complications associated with its

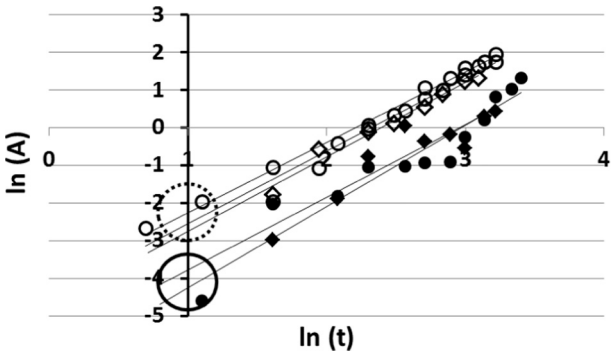

Fig. 11. Natural log plot of absorbance versus time in seconds obtained from subjects with BG < 120 mg dL^{-1} and no underlying conditions. Only trials where n ~ 2 was observed are included. Open circles represent data for 34 year old female, open diamonds are for 54 year old male, closed circles are for 70 year old male, closed diamonds are for 73 year old female. The dashed circle indicates the vertical intercept grouping where $t = 1$ s for the younger subjects whereas the solid circle indicates the corresponding grouping for the older subjects. Exhalation rate was 2.0 L min^{-1} and a humidified purge was employed in all cases. All but the open circle data employed a 7 mil optode. The less negative intercept for the younger subjects indicates higher lung tissue permeability.

interpretation, we provide preliminary results from these trials in Fig. 11. Only those trials for which n ~ 2 was achieved are included. In addition to the 34 year old female subject from whom Fig. 8 was generated, we obtained satisfactory results for three other subjects: a 54 year old male, a 73 year old female, and a 70 year old male. For comparison purposes, C_0 may be set to 1 ppm for this non-diabetic set of subjects.

Fig. 11 suggests that the two older subjects group together with an intercept, $\ln(B_nC_0)$, that differs from that of the two younger subjects. The physiological implication of this data requires careful investigation of differences in parameters k_c and V_0 found in Eq. (18). While k_c is associated with capillary permeability, V_0 is associated with the anatomical conditions of the subjects. For example, the internal pressure required to maintain a forced exalation of 2 L min^{-1} may result in changes to the anatomical dead space (comprised of the nose, trachea, and bronchi) that differ from one group to the other due to, for example, tissue elasticity. The total lung volume, V_0, consists of both this dead space and the respiratory zone (comprised of respiratory bronchioles, alveolar duct, alveolar sac, and alveoli). Thus, before any assertions can be made regarding tissue permeability, an independent method of assessing total lung volume during forced exhalation is needed. One approach we are currently investigating is to use a second exhaled VOC (e.g., formaldehyde [18]) to normalize the response and factor out lung volume.

4. Conclusions

This work reports on the construction and operational characteristics of a device capable of measuring the time-dependence of exhaled breath acetone concentration in real time. Acetone sensing is achieved utilizing a catalytically-driven membrane reaction with acetone to produce a color which is then read by measuring reflected light in RGB. The highly sensitive sub-ppm optode response has sufficiently fast time resolution (~1 s) to permit in-situ measurement of the accumulation of acetone in a flow-through sample chamber during the brief time period (~40 s) that is typical of breath exhalation. The use of this flow-through sample chamber for in-situ chemical analysis of an acetone flow stream having constant inlet concentration yields a time dependence in the optical response that varies from $t^{1/2}$ to t for at least 40 s. The precise power law is shown to depend on whether acetone accumulation is limited by the sample chamber or the membrane as well as on the time-dependence of the inlet concentration. A t^2 dependence is observed in the absence of membrane mass transport resistance that is correlated to a linear increase in breath acetone concentration during forced exhalation. This behavior has never previously been reported and is here attributed to lung physiology through a material balance entailing blood acetone partitioning into and through the capillary wall/lung tissue structure. Such partitioning in the respiratory zone is more rapid than the forced acetone exhalation rate and results in a linear time-dependent increase in the average concentration in the total lung volume, which includes the anatomical dead space. Lung tissue permeability results are shown to be consistent with independent material parameter data. A preliminary assessment is presented on the impact of age on lung physiology.

Declaration of Competing Interest

The authors declare that they have no known competing financial interests or personal relationships that could have appeared to influence the work reported in this paper.

Acknowledgements

This work was supported by the U.S. National Science Foundation (Grant CBET- 1836556) and the University of Cincinnati and is gratefully acknowledged.

References

[1] N. Alizadeh, H. Jamalabadi, F. Tavoli, Breath acetone sensors as non-invasive health monitoring systems: a review, IEEE Sensors J. 20 (2020) 5–31.
[2] Q.C. Zhang, W.L. Yan, L. Jiang, Y.G. Zheng, J.X. Wang, R.K. Zhang, Synthesis of Nano-praseodymium oxide for Cataluminescence sensing of Acetophenone in exhaled breath, Molecules 24 (2019).
[3] D. Wang, S.M. Huang, H.J. Li, A.Y. Chen, P. Wang, J. Yang, X.Y. Wang, J.H. Yang, Ultrathin WO3 nanosheets modified by g-C3N4 for highly efficient acetone vapor detection, Sensors Actuators B-Chem. 282 (2019) 961–971.
[4] T.P.J. Blakie, J. Couper, G. Hancock, P.L. Hurst, R. Peverall, G. Richmond, G.A.D. Ritchie, D. Taylor, K. Valentine, Portable device for measuring breath acetone based on sample preconcentration and cavity enhanced spectroscopy, Anal. Chem. 88 (2016) 11016–11021.
[5] V. Saasa, M. Beukes, Y. Lemmer, B. Mwakikunga, Blood ketone bodies and breath acetone analysis and their correlations in type 2 diabetes mellitus, Diagnostics 9 (2019).
[6] W.W. Li, Y. Liu, Y. Liu, S.Q. Cheng, Y.X. Duan, Exhaled isopropanol: new potential biomarker in diabetic breathomics and its metabolic correlations with acetone, RSC Adv. 7 (2017) 17480–17488.
[7] J.H. Leopold, R.T.M. van Hooijdonk, P.J. Sterk, A. Abu-Hanna, M.J. Schultz, L.D.J. Bos, Glucose prediction by analysis of exhaled metabolites - a systematic review, BMC Anesthesiol. 14 (2014).
[8] T.P.J. Blaikie, J. Couper, G. Hancock, P.L. Hurst, R. Peverall, G. Richmond, G.A.D. Ritchie, D. Taylor, K. Valentine, Portable device for measuring breath acetone based on sample preconcentration and cavity enhanced spectroscopy, Anal. Chem. 88 (2016) 11016–11021.
[9] J. Sorocki, A. Rydosz, A prototype of a portable gas analyzer for exhaled acetone detection, Appl. Sci.-Basel 9 (2019).
[10] A.D. Worrall, Z. Qian, J.A. Bernstein, A.P. Angelopoulos, Water-resistant polymeric acid membrane catalyst for acetone detection in the exhaled breath of diabetics, Anal. Chem. 90 (2018) 1819–1826.
[11] A.P. Angelopoulos, S.M. Ayyadurai, J.A. Bernstein, D. Kanter, Optical Sensor Based on PFSI Membrane Comprising Associated Benzene 1,3-Diol for Detecting Target Compounds and Method Therof, in: US 9,921,167, University of Cincinnati, United States, 2018.
[12] A.D. Worrall, Immobilization of organic molecules within perfluorosulfonic acid membranes for optical sensing in humid environments, Chemical Engineering Program, University of Cincinnati, Cincinnati, OH, 2014.
[13] C.M. Hansen, The significance of the surface condition in solutions to the diffusion equation: explaining “anomalous” sigmoidal, case II, and super case II absorption behavior, Eur. Polym. J. 46 (2010) 651–662.
[14] D. Hansen, J.R. Brewer, J. Eiler, N.M. Komjani, K. Hansen, E. Thormann, Water diffusion in polymer composites probed by impedance spectroscopy and time-resolved chemical imaging, Acs Appl. Polym. Mater. 2 (2020) 837–845.
[15] J. Crank, The Mathematics of Diffusion, Second edition, Oxford University Press, New York, 1975.
[16] H. Takeuchi, Y. Mano, S. Terasaka, T. Sakurai, A. Furuya, H. Urano, K. Sugibayashi, Usefulness of rat skin as a substitute for human skin in the in vitro skin permeation study, Exp. Anim. 60 (2011) 373–384.
[17] G. Cocchi, M.G. De Angelis, F. Doghieri, Solubility and diffusivity of liquids for food

and pharmaceutical applications in crosslinked polydimethylsiloxane (PDMS) films: I. Experimental data on pure organic components and vegetable oil, J. Membr. Sci. 492 (2015) 600–611.
[18] S. Ravi, A.D. Worrall, A.P. Angelopoulos, Formaldehyde detection and removal in direct alcohol fuel cell effluent, Abstracts of Papers of the American Chemical Society, 246 2013.

Ms. Ulzii-Orshikh Badmaarag received her Masters of Science Degree in Chemical Engineering in 2020 from the Department of Chemical and Environmental Engineering at the University of Cincinnati. She holds a Bachelor of Engineering Degree in Food Science Technology and Engineering obtained in 2011 from Tianjin University. Ms. Badmaarag has extensive experience as a translator in science and technology as well as interacting with subjects on small-scale clinical trials involving non-invasive breath acetone measurement.

Dr. Jonathan A. Bernstein is Professor of Clinical Medicine in the Department of Internal Medicine, Division of Immunology/Allergy Section at the University of Cincinnati Medical Center and partner of the Bernstein Allergy Group and Clinical Research Center. He received his MD from the University of Cincinnati College Of Medicine in 1985. He completed his residency training in Internal Medicine at the Cleveland Clinic Hospital from 1985 to 1988 and his Allergy/Clinical Immunology training at Northwestern University from 1988 to 1990. His current research involves environmental health effects and interventions in the home and workplace related to asthma and rhinitis in addition to the investigation of asthma, angioedema/chronic urticaria, atopic dermatitis genomics/transcriptomics and novel therapies. Dr. Bernstein is a DIA certified investigator with extensive experience conducting multicenter and physician initiated clinical therapeutic trials. He is editor-in-chief of the *Journal of Asthma*.

Dr. Reza Shekarriz is an innovator and entrepreneur engaged in various aspects of small high technology business development including strategic planning, targeted technology development, academic and industrial partnership, product development and deployment, intellectual property development and protection, and seed-to-market implementation of new technologies. He received his Ph.D. in Mechanical Engineering from Washington State University in 1988. He was a post-doctoral fellow at the Johns Hopkins University from 1989 to 1991 and from there he went on to join PNNL and was a staff scientist prior to leaving the laboratory in 1998 to pursue entrepreneurial activities. He was a Principal engineer and Senior Director in several start-up companies, namely MesoSystems, Acoustic Biosystems, Greentheme Technologies, Yainax Medical, and Fluid Analytics. In 2008, Fluid Analytics formed a partnership with ABSOGER, SAS in France to commercialize technologies for sensing and control of volatile gases in the postharvest market. Currently, a spin off from Fluid Analytics, namely Exhalix, LLC, is focused on development of miniature sensors for health monitoring.

Dr. Anastasios P. Angelopoulos is Professor and Head of the Department of Chemical and Environmental Engineering at the University of Cincinnati (UC). He holds a Ph.D. degree in Chemical Engineering from Princeton University (1996) and M.S. and B.S. degrees, both in Chemical Engineering, from Tufts University (1988 and 1984, respectively). Prior to joining UC 14 years ago, he was Staff Engineer at the IBM Corporation in Endicott, NY, Assistant Professor in Chemistry at the University of Massachusetts Lowell, and Senior Materials Scientist at the General Motors Fuel Cell Research and Development Center in Honeoye Falls, NY. He also spent 4 years as Research Associated at the U.S. Army Materials Technology in Watertown, MA where he conducted research on barrier membrane materials. Dr. Angelopoulos conducts research on chemical sensing materials for medical diagnostics and occupational settings as well membrane-electrode assemblies for alternative energy development.